Geochemical Evolution and Groundwater Flow System in Batujajar Groundwater Basin Area, West Java, Indonesia

Rudy Suhendar[1,2], M. Sapari Dwi Hadian[1], Budi Muljana[1], Taat Setiawan[2], and Hendarmawan[1]

[1]Faculty of Geological Engineering, Padjadjaran University
Jln. Raya Bandung-Sumedang Km.21 Jatinangor, Indonesia 45363
[2]Geological Agency, Ministry of Energy and Mineral Resources of the Republic of Indonesia
Jln. Diponegoro No. 57 Bandung, Indonesia

Corresponding author: hidrosetiawan@gmail.com

Abstract - Batujajar and its surrounding areas, situated in the west of the Bandung Basin, are geologically composed of various Tertiary rock formations with complex fold and fault systems. Springs and drilled wells in sandstone aquifers, tuffaceous sand, and tuffaceous breccias mark the development of their aquifer systems. This study aimed to determine the characteristics of the hydrogeochemistry by analyzing major ions and stable isotopes (^{18}O and ^{2}H) of thirty-four hydrogeological objects. The groundwater flow pattern in this area is controlled by northwest-southeast lineament, as indicated by the emergence of springs along the transition zone between areas with high and low lineament density. In order of dominance, the groundwater facies are as follows:$Ca-Mg-HCO_3$>$Ca-HCO_3$>$Ca-Na-Mg-HCO_3$>$Na-Ca-HCO_3$. Hydrochemical evolutions were detected from the change of cations from Ca^{2+} to Mg^{2+} and then Na^+, and this is believed to be the product of cation exchange and dissolution of silicate minerals. However, evolutions toward anion changes were not apparent yet, meaning that HCO_3^- ions still prevail, or in other words the groundwater flow system is local. Nevertheless, the geological and hydrogeochemical analyses, along with the relative compositions of stable isotopes, revealed that the groundwater had three systems, namely shallow, intermediate, and deep groundwater flows; all of which were segmented in three subgroundwater basins (Sub-GWB). Aquifer systems with shallow to intermediate groundwater flow were found in Sub-GWB-A, Sub-GWB-B, and Sub-GWB-C, while the other ones with deep groundwater flow system were identified in Sub-GWB-B and Sub-GWB-C.Fracture system has an important role as a connector between recharge system in hilly areas and discharge system in plain areas.

Keywords: hydrochemistry, stable isotope, groundwater flow, Batujajar, Bandung

Introduction

Geographically, the studied area is located in the west of Bandung City, the capital of West Java Province, Indonesia (Figure 1). According to the Regulation of the Minister of Energy and Mineral Resources Number 2 of 2017, the researched area is part of the Batujajar Groundwater Basin. This claim indicates a series of hydrological process in the area, including recharge, flow or drainage, and groundwater extraction from one or more suitable aquifers (Mandel, 1981; Todd, 1984) that are bordered by hydrogeological boundaries (Sophocleous, 2004). Toth (2009) suggests that in a large
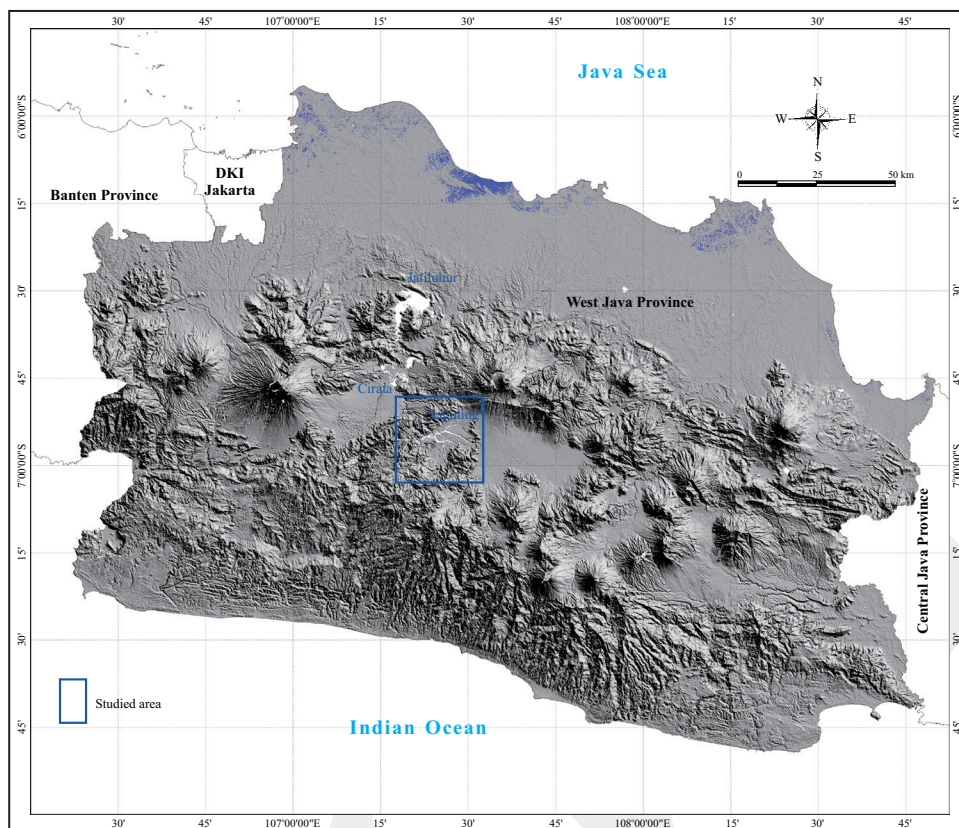
Figure1. Location of the studied area lies in the west of Bandung City, West Java, Indonesia.

groundwater basin, the anion facies systematically change from HCO_3^- to SO_4^{2-}. At last, Cl^-, based on the Mandel classification (1981), the hydrogeological system in the studied area is of folded or faulted sedimentary rocks. While according to Soetrisno (1982), it is a fissure aquifer with low productivity and scarce groundwater. A discussion of whether a groundwater basin in a folded sedimentary rock with low productivity has the characteristics of groundwater chemical evolution as explained by Toth (2009) is thereby interesting.

This study determines the geochemical evolution of groundwater and its relationship with groundwater flow systems by hydrochemical analysis and stable isotopes (^{18}O and ^2H). There have been many studies of Bandung Basin and its surrounding areas, but none of them is Batujajar Groundwater Basin. IWACO and Waseco (1991) stated that most of the aquifers in Bandung Basin were related to one of the debris flows from Mount Tangkuban Parahu that formed the Bandung and Cimahi fan deposits or to the "fluvio-volcanic"

deposits that composed the fan deposits on the edge of an ancient lake. The fan deposits in the west (Cimahi) are the essential source of groundwater flow to Batujajar Basin. IWACO and Waseco (1991) had found brackish groundwater in one of the production wells in the plain area of Batujajar at a depth of 130 m, which is an indication of Tertiary sediments lying underneath. Sunarwan (1997) stated that Padalarang and its surrounding areas had a volcanic aquifer system composed of alternations of breccias, sandy tuff, and andesitic lava of Cibeureum Formation.

There has been a significant amount of research of stable isotopes in Bandung-Soreang Groundwater Basin, specifically in the middle of the basin. According to Geyh (1991), the recharge zone of the groundwater in the Bandung plain is at an altitude of 1,050 - 1,300 m asl. and is located more or less in the north of Lembang. Matahelumual and Wahyudin (2010) divide the recharge areas of aquifers at the depths of 70 - 200 m into two, namely at an elevation of upwards

of 1,200 m asl. or above the Lembang fault zone and at an altitud

e between 900 m and 1,200 m asl. or above the Lembang fault zone. In contrast, Delinom (2009) believes that the Lembang Fault can restrict the groundwater movement.

Geological Setting

Based on Sudjatmiko (1972 and 2003), Silitonga (1973), Koesmono (1976), and Koesmono, *et al.* (1996), the studied area geologically comprises various rock formations, including Tertiary-aged sedimentary rocks deposited in the marine environment, rocks produced by Tertiary to Quaternary volcanoes, and alluvium (Figure 2). The oldest sedimentary rocks are claystone (Tomc) and limestone (Toml) members of the Oligocene Rajamandala Formation, which are intruded by dacitic-andesitic rocks. Unconformably overlying them are sedimentary rocks, namely the Miocene rock units from the Beser Formation (Tmbe), the Sandstone Member of the Cilanang

Formation (Tmtjs), the Breccias and Sandstone Member of the Citarum Formation (Tmtb), and the Sandstone and Siltstone Member of the Citarum Formation (Tmts).

Lying on the sedimentary rock units are unconformable deposits, comprising of rocks produced by Pliocene volcanoes such as the Andesitic Lava Formation that contains pyroxene (Tpa) and tuffaceous breccia, lava, sandstone, and conglomerate (Tpb). On top of the Pliocene volcanic rocks, several rock formations are deposited conformably, including Quaternary alluvial rocks of volcanic products and mixed sedimentary rocks which are breccias, lava, and undifferentiated volcanic deposits (Qv), volcanic fan deposits which are laharic breccias (Qvf) alluvium consisting of clays, silts, sand, pebbles, and gravels (Qa), and tuffaceous lake deposits (Ql).

The formation of geological structures in the studied area is attributable to the west-east Java geanticline, which were formed at the end of Paleogene, *i.e.* when the uplift of the basement is
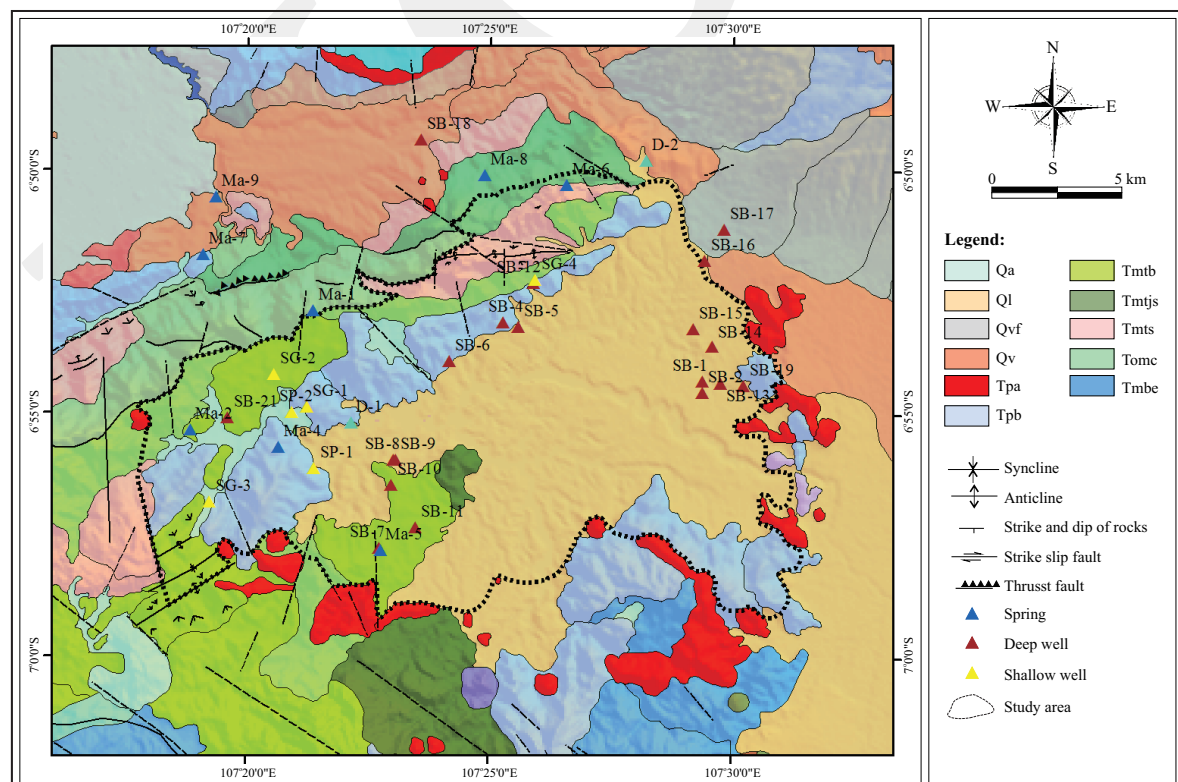

Figure 2. Geological map of the studied area and its surrounding areas (modified from Sudjatmiko, 1972 and 2003; Silitonga, 1973; Koesmono *et al*,, 1996).

accompanied by several folds, especially in the Cimandiri Valley (Bemmelen, 1949). The axis of the fold is east-west. According to Sudjatmiko (1972), Silitonga (1973), Koesmono (1976), Koesoemadinata and Hartono (1981), Dam and Suparan (1992), Dam (1994), and Koesmono *et al.* (1996) the geological structures in Bandung include the west-east Lembang Normal Fault, the Rajamandala Reverse Fault Zone, and several east-west normal faults in the south of Bandung Plain and Batujajar.

METHODS

Hydrogeological Observation

Samples consisting of water from deep wells, springs, and shallow wells were taken on April - May 2018 for hydrochemical and stable isotope (^{18}O and ^{2}H) analyses. Some parameters like temperature, pH, and electrical conductivity (EC) were examined in the field with the Portable Lamotte Water Test Kit.

Morphological Lineament Analysis

The morphological lineaments were extracted from Terrasar-X SRTM (Shuttle Radar and Topography Mission) images with 30 m resolution and processed in PCI Geomatica software to generate lineament patterns. Afterwards, these patterns were subjected to lineament count density analysis in ArcGis 10.3, which aimed to determine the density and distribution pattern of the lineaments (Kim, 2003). The output was a map of lineament count density, expressed in n/km^2 (count of lineaments/km^2).

Hydrochemical Analysis of Major Ions

The major ions Ca^{2+}, Na$^+$, Mg^{2+}, K$^+$, HCO$_3^-$, SO$_4^{2-}$, and Cl$^-$ were analyzed in the laboratory. The presence of Ca^{2+}, Na$^+$, Mg^{2+}, and K$^+$ was identified in the Dionex ICS-1500 Ion Chromatography System, and SO$_4^{2-}$ and NO$_3^-$ were detected in Varian Cary 100 UV-Visible Spectrophotometers. Meanwhile, Cl$^-$ and HCO$_3^-$ contents were measured by argentometry and alkalinity by titration, respectively. The quality of the laboratory analyses was represented by charge-balance error (CBE) (Freeze and Cherry, 1979). The test results were accepted when the CBE is < 5% (Al Charideh, 2011; Wu *et al.*, 2013; Yuan *et al.*, 2017).

Stable Isotope Analyses (^{2}H and ^{18}O)

The stable isotope analyses were performed in the hydrochemical laboratory of the Centre for Groundwater and Environmental Geology, the Geological Agency of Indonesia. The isotopic compositions, *i.e.* ^{18}O and ^{2}H, in water samples were measured in Instrument Picarro L-2130-i. The abundance of ^{18}O and ^{2}H molecules in water was not measured absolutely, but relatively to a predefined standard. The relative abundances of HD^{16}O and H$_2$^{18}O molecules are each termed the relative abundance of deuterium (δD) and ^{18}O (δ^{18}O). These measures were comparable to the international standard SMOW (Standard Mean Ocean Water) (Eriksson, 1983; Clark, 2015).

RESULTS

Fracture Systems

From the hydrogeological point of view, fracture zones (joints, faults) significantly contribute to controlling the hydrogeological system in solid rocks, because they have excellent secondary permeability and porosity development (Parizek, 1967, in Fetter, 2001). Groundwater tends to flow through fracture zones, which are morphologically indicated by lineaments as fracture traces. According to Singhal and Gupta (1999), morphological lineament is an expression of planes of discontinuities in rocks, comprising fractures, joints, and faults; all of which are the morphological parts of valleys developing between ranges of hills.

The morphological lineaments in the studied area were extracted from 30m-resolution SRTM imagery, which successfully identified about 320 lineaments (Figure 3). Based on the rose diagram analysis, they form a pattern in the directions of N 270° - 320°E, with a mean vector of N131°E or north-southeast direction. Morphological lineament density is a quantification of the spatial distribution of morphological lineaments that is
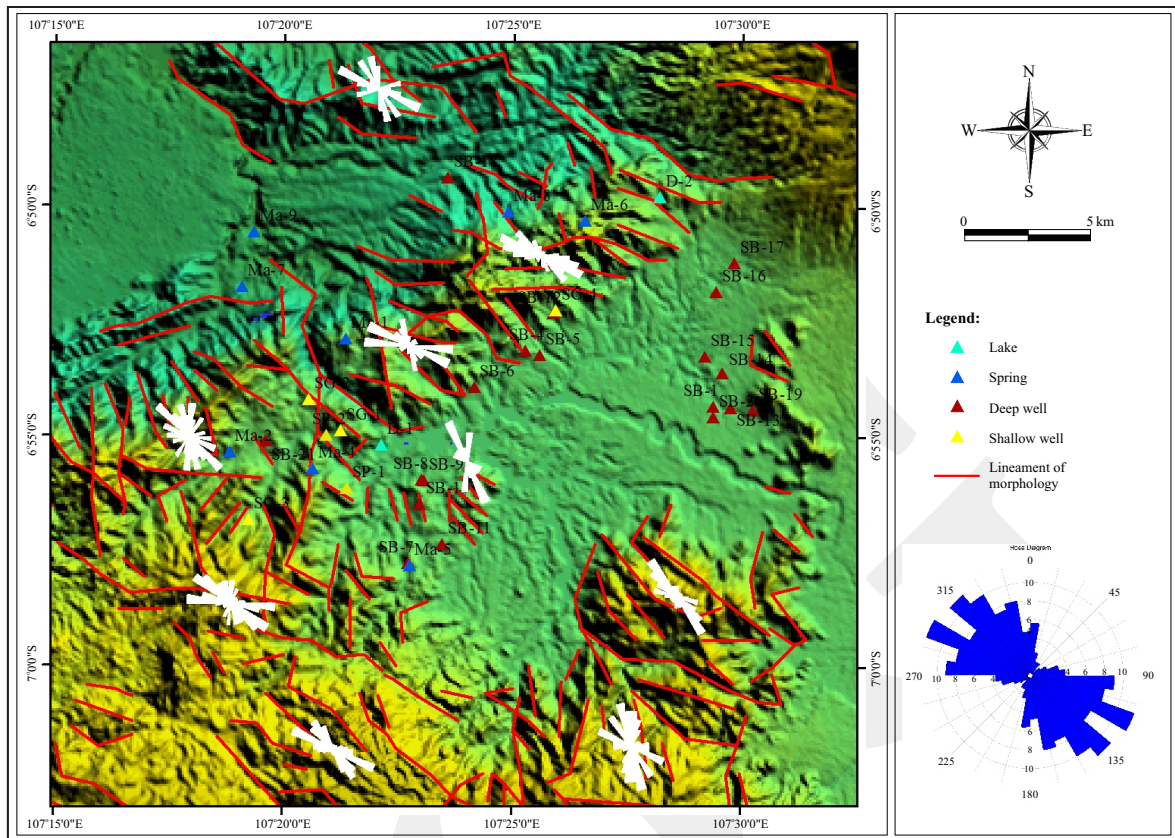
Figure 3. Extraction of morphological lineament and the rose diagram results of the lineament directions of N 270° - 320°E with a mean vector of N131°E.

useful to determine their concentration zone and distribution pattern. The analysis results show that the density has various directions and increases with elevation (hills). Springs are located at the geological borders formed by adjacent low- and high-density zones (Figure 4). In other words, their emergences are situated between areas with developed fracture system (high lineament density) and areas with less developed fracture system (low lineament density).

Hydrochemistry

According to Schwartz and Zang (2003), mineral constituents of rocks are dissolved in water and form dissolved ions. The average major ion compositions of thirty-three water samples, consisting of twenty water samples from shallow wells, eight from springs, and five from shallow well, are presented in Table 1. The charge-balance errors (CBEs) of the analysis results range between 1.0 and 4.8% with an average of 3.11%.

The hydrochemical analysis of the major ions reveals that, in order of abundance, the cations in water samples from deep wells, springs, and shallow wells are $Ca^{2+}>Na^+>Mg^{2+}$, while the anions in water samples from deep and shallow wells are $HCO_3^->Cl^->SO_4^{2-}$ and in those collected from the springs are $HCO_3^->SO_4^{2-}>Cl^-$. Comparing with springs and shallow wells, the groundwater samples from the deep wells had the average higher contents of Na^+, K^+, HCO_3^-, Cl^-, and SO_4^{2-}. Also, deep wells have a higher electrical conductivity (EC) than shallow wells and springs. Based on this description, a high EC is attributable to the enrichments of Na^+, K^+, HCO_3^-, Cl^-, and SO_4^{2-}.

The hydrochemical analysis is graphically presented in the Piper diagram (Figure 5). The water in shallow wells has four hydrochemical facies, namely $Ca-Mg-HCO_3$, $Ca-HCO_3$, $Ca-Na-HCO_3$, and $Mg-Na-HCO_3$. Springs have three hydrochemical facies, namely $Ca-Mg-HCO_3$ (in two samples), $Ca-HCO_3$ (5), and
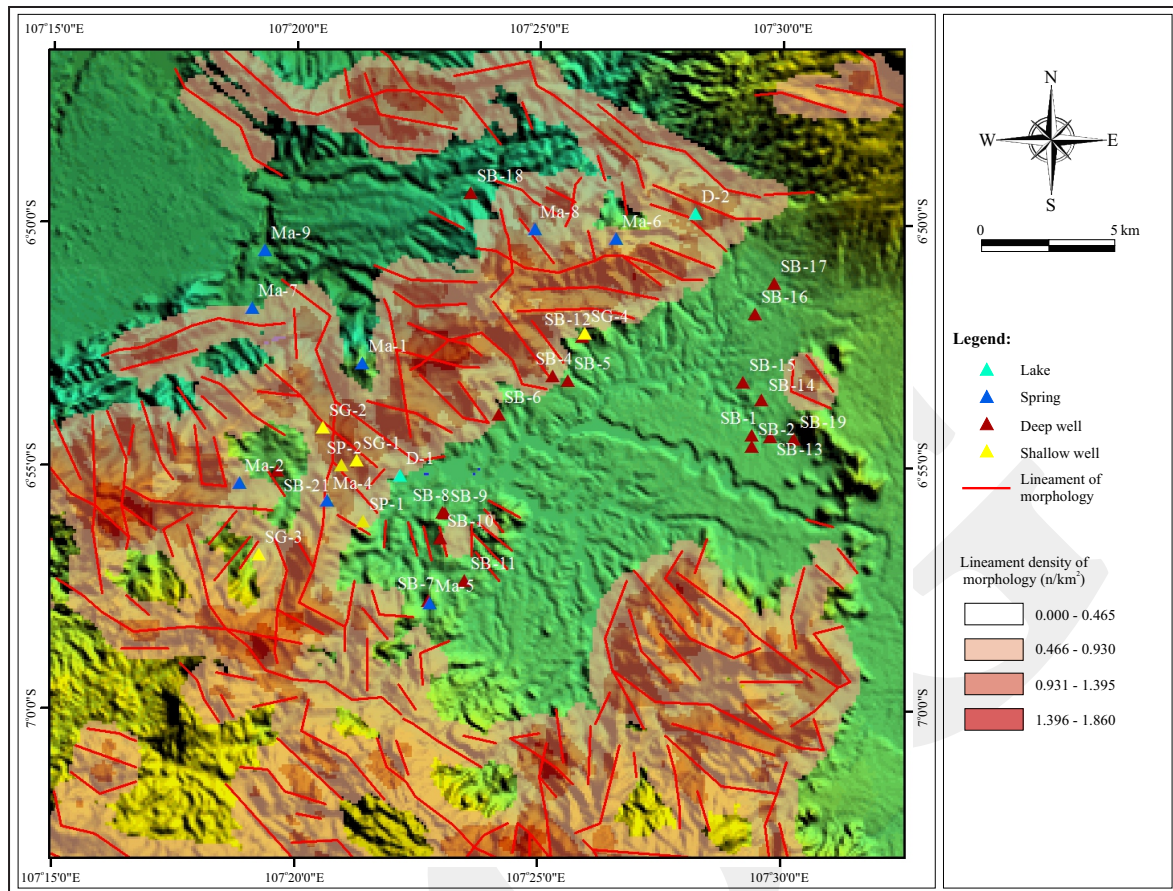
91

Figure 4. Spatial distribution of the morphological lineament density in the studied area having various directions and increasing with elevation.

Table 1. Range and the Average of the Major Ion Compositions of Water Samples in Studied Area

Parameters	Deep Wells			Springs			Shallow Wells		
	Min.	Max.	Avg.	Min.	Max.	Avg.	Min.	Max.	Avg.
EC	208	686	429	149.77	477.48	283.32	123.93	477.48	259.87
pH	6.55	8.03	7.21	6.75	7.26	6.95	6.56	7.28	6.96
Ca^{2+}	19.73	89.5	45.80	19.38	61.73	41.49	16.88	31.56	25.02
Mg^{2+}	5.48	25.91	13.75	0.33	21.42	8.74	0.83	35.87	12.32
Fe^{3+}	0.00	2.80	0.68	0.00	0.86	0.15	0.00	0.32	0.12
K^+	1.27	14.59	4.12	0.39	1.77	0.96	0.59	3.40	2.08
Na^+	8.9	96.43	31.85	8.79	15.40	11.16	9.17	35.32	15.13
HCO_3^-	117.08	373.48	251.29	69.31	305.46	189.79	38.50	256.69	144.52
Cl^-	6.30	83.29	19.89	5.13	9.87	6.81	5.92	37.50	15.11
$SO_4^=$	0.00	51.00	12.53	0.50	22.70	10.61	0.60	32.50	13.52
NO_3^-	0.00	23.20	5.36	0.00	5.00	2.15	0.30	13.90	5.30

$Ca-Na-HCO_3-SO_4$ (1). As for the deep wells, they have seven hydrochemical facies, namely $Ca-Mg-HCO_3$ (in seven samples), $Ca-Mg-Na-HCO_3$ (4), $Ca-Na-Mg-HCO_3$ (3), $Ca-Na-HCO_3$ (1), $Na-Ca-Mg-HCO_3$ (1), $Na-Ca-HCO_3$ (3), and $Ca-Na-HCO_3-Cl$ (1).

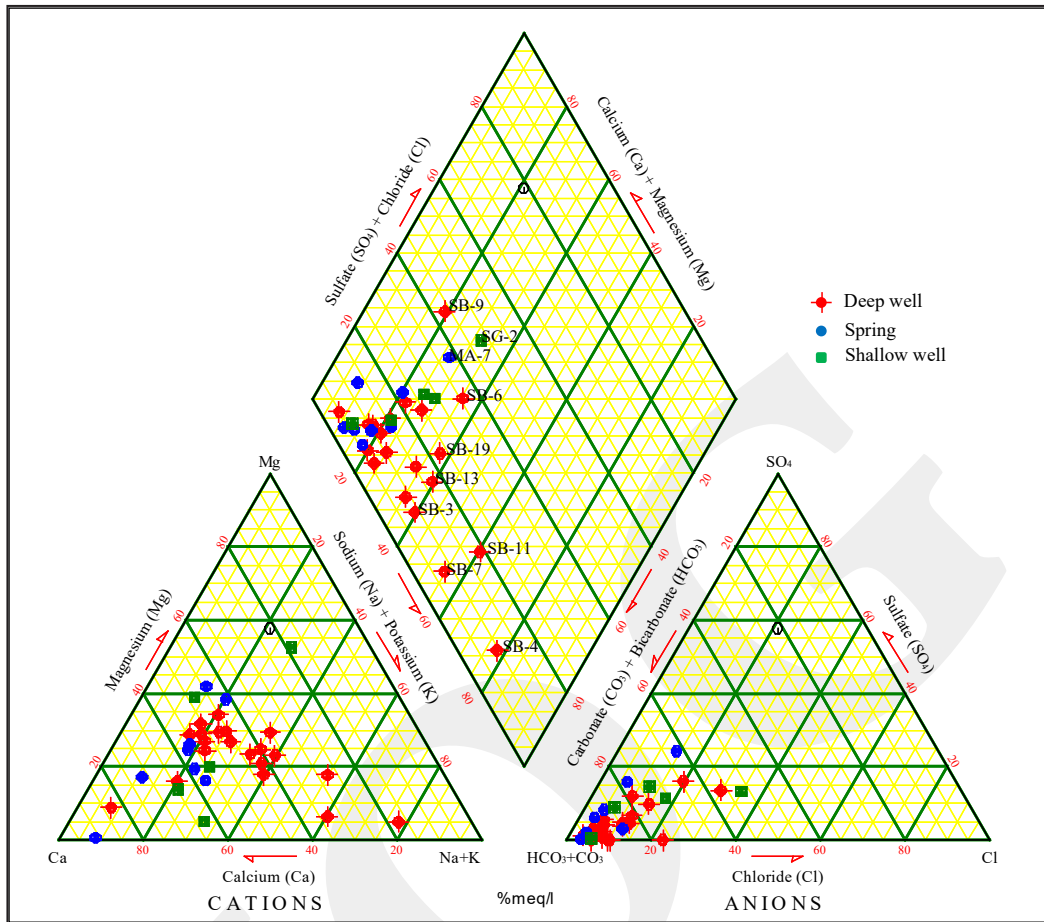Based on the groundwater facies, the water samples from the deep wells (SB) exhibit a

Figure 5. Piper diagram showing the water samples from deep wells exhibited the enrichment of Mg^{2+} and Na^+ after Ca^{2+} as the dominant ion.

change in their cation composition, *i.e.* the enrichment of Mg^{2+} and Na^+ after Ca^{2+} as the dominant ions. Moreover, Na dominates SB-3, SB-4, SB-7, and SB -11. The Na-Ca-HCO_3 groundwater in the Piper diagram is located separately from the other groundwater facies, indicating that the groundwater chemically evolves as it moves from the recharge to the discharge areas. Such evolution is attributable to changes in groundwater cations, *i.e.* from Ca^{2+} to Mg^{2+}, as the consequence of cation exchange (Sposito, 1989, in Kehew, 2001).

Hydrochemical Process

The Gibbs diagram (Gibbs, 1970) is an effective method for identifying hydrogeochemical processes in aquifers (Yuan *et al*., 2017). It is a scattered plot of TDS against Na/(Na+Ca) for cations and Cl/(Cl+HCO_3) for anions. The groundwater samples are all within the Rock

Dominance or Rock Weathering zone (Figure 6), meaning that the hydrogeochemical process in the studied area is mainly mineral dissolution due to a high interaction between groundwater and aquifer rocks. This level of groundwater interaction is also shown by Na enrichment, which indicates a dominant cation exchange in SG-4, SB-3, SB-4, SB-11, and SB-7.

The ratio of (Ca+Mg)-(HCO_3+SO_4) to Na-Cl is used to evaluate the cation exchange process in groundwater (Wang *et al*., 2015). On the bivariate chart, these two parameters demonstrates that a cation exchange mostly occurs in samples numbers SB-3, SB-4, SB-7, SB-11, and SB-13 (Figure 7). Accordingly, the residence time or the interaction process between groundwater and rock constituents of aquifers in these groundwater samples is particularly longer than in other samples. A strong determination between the
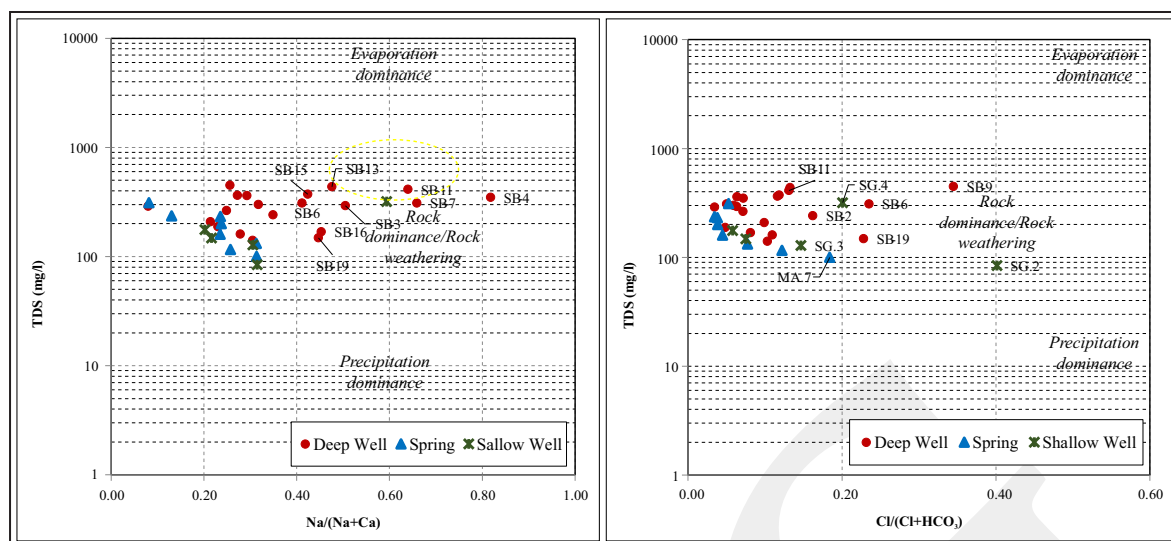
Figure 6. Gibbs diagram showing all the water samples are situated within the rock dominance zone.
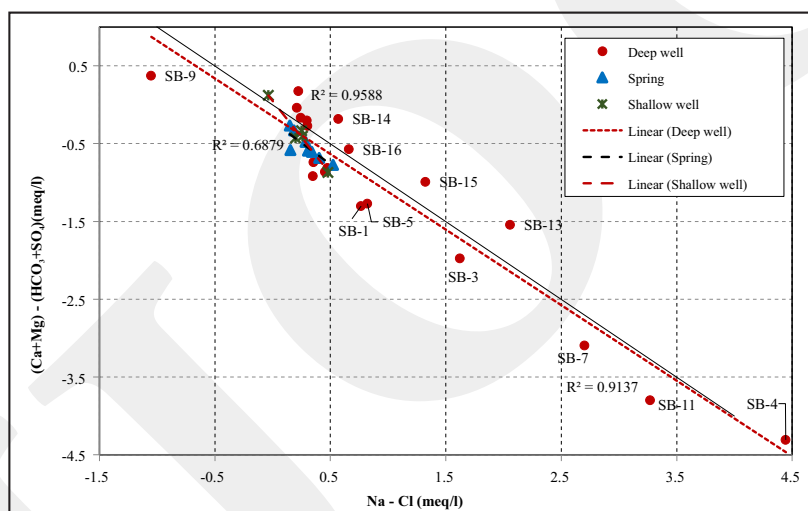

Figure 7. Plots of (Ca+Mg)-(HCO$_3$+SO$_4$) *vs*. Na-Cl showing the cation exchange mostly occurs in samples numbers SB-3, SB-4, SB-7, SB-11, and SB-13.

two parameters is found in groundwater samples from shallow wells (R^2= 0.958) and deep wells (R^2= 0.914). Meanwhile, the samples collected from the springs yield R^2= 0.687. In other words, the cation exchange in both confined and unconfined aquifers exhibits a dominant influence on the hydrogeochemical characters of groundwater.

Apart from the ratio of (Ca+Mg)-(HCO$_3$+SO$_4$) to Na-Cl, a decrease in Ca^{2+} content and enrichment of Na$^+$ can also demonstrate the occurrence of cation exchange (Schoeller 1977; Hem 1992). The plotting of EC points against Ca/Na ratio

(Figure 8) identifies a dominant cation exchange process in SB-3, SB-4, SB-6, SB-7, SB-11, SB-13, SB-15, SB-16, SB-19, and SG-4. These groundwater samples also have relatively high electrical conductivities, especially in SB-11, SB-13, and SB-15, suggesting that the cation exchange is fundamental in modifying the chemical-physical properties of groundwater.

The plotting of Ca/Na and HCO$_3$/Na molar ratio can distinguish between the dissolutions of silicate and carbonate rocks (Gaillardet *et al.*, 1999). In this study, the plots show that almost all water samples are in the vicinity of the silicate
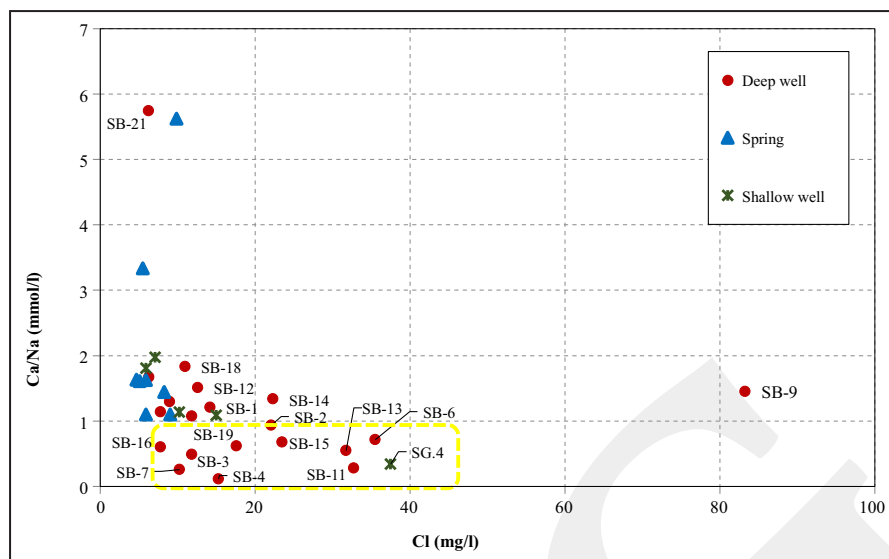
Figure 8. Plots of Ca/Na ratio *vs*. Cl of groundwater samples showing the dominant cation exchange process in SB-3, SB-4, SB-6, SB-7, SB-11, SB-13, SB-15, SB-16, SB-19, and SG-4.

dissolution zone (Figure 9). Silicate dissolution is natural because the studied area is also composed of siliciclastic sedimentary rock formations, including sandstone. Based on the chart of Ca/Na and HCO_3/Na molar ratio, silicate dissolution occurs most intensively in water samples numbers SB-3, SB-4, SB-6, SB-7, SB-11, SB-13, SB- 15, SB-16, SB-19, and SG-4.

Stable Isotopes

The $\delta^{18}O$ and $\delta^{2}H$ analysis results of twenty-eight samples from deep wells (SB), shallow wells (SP), and springs (Ma) are presented in Tables 2 and 3. The $\delta^{18}O$ and $\delta^{2}H$ compositions in springs and deep wells have the similar average, but higher variation in springs. The coefficient of variance (CV) of ^{18}O and ^{2}H levels in springs (Table 3) is higher than in deep wells (Table 2). In another
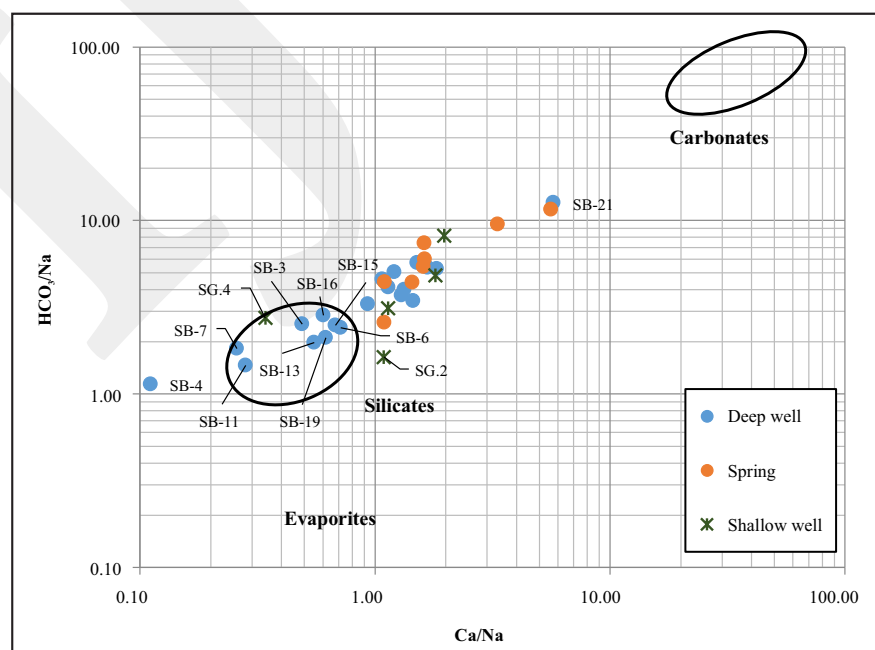

Figure 9. Plots of HCO_3/Na against Ca/Na showing the silicate dissolution occurs most intensively in water samples numbers SB-3, SB-4, SB-6, SB-7, SB-11, SB-13, SB- 15, SB-16, SB-19, and SG-4.

Table 2. Compositions of $\delta^{18}O$ and δ^2H in the Groundwater Samples of Deep Wells

No.	Codes	X	Y	$\delta^{18}O$	SD ^{18}O	δ^2H	SD ^2H
1	SB-1	775125	9235988	-6.562	0.255	-42.109	0.623
2	SB-2	775133	9235562	-6.569	0.245	-40.673	0.589
3	SB-4	767553	9238237	-6.681	0.248	-41.887	0.611
4	SB-6	765525	9236773	-6.514	0.238	-41.025	0.642
5	SB-7	762839	9229696	-6.452	0.242	-39.376	0.653
6	SB-8	763388	9233041	-6.494	0.255	-40.965	0.626
7	SB-10	763317	9232075	-6.845	0.244	-42.312	0.661
8	SB-11	764232	9230474	-6.090	0.247	-37.402	0.633
9	SB-12	768704	9239727	-6.019	0.260	-38.324	0.641
10	SB-13	775819	9235914	-6.266	0.245	-39.340	0.649
11	SB-14	775501	9237327	-6.585	0.250	-40.875	0.633
12	SB-15	774780	9237988	-6.112	0.239	-40.248	0.601
13	SB-16	775230	9240564	-7.308	0.245	-45.553	0.618
14	SB-17	775965	9241739	-7.446	0.253	-46.210	0.650
15	SB-18	764459	9245178	-6.229	0.241	-38.345	0.577
16	SB-19	776696	9235817	-7.403	0.252	-46.379	0.643
17	SB-20	760122	9235039	-6.254	0.242	-38.179	0.561
18	SB-21	757106	9234636	-6.161	0.247	-37.606	0.633
19	SP-1	760383	9232717	-6.311	0.251	-40.092	0.650
20	SP-2	759542	9234854	-6.144	0.241	-35.828	0.636
Avg.				-6.52		-40.64	
Std. Dev.				0.43		2.89	
CV				-6.62		-7.10	

Table 3. Compositions of $\delta^{18}O$ and δ^2H in the Groundwater Samples of Springs

No.	Codes	X	Y	$\delta^{18}O$	SD ^{18}O	δ^2H	SD ^2H
21	Ma-1	760344	9238709	-6.848	0.253	-41.434	0.657
22	Ma-2	755676	9234179	-6.379	0.260	-37.876	0.616
23	Ma-4	759020	9233511	-6.715	0.241	-40.913	0.661
24	Ma-5	762897	9229596	-6.713	0.262	-41.004	0.626
25	Ma-6	769975	9243451	-7.387	0.249	-45.475	0.683
26	Ma-7	756168	9240814	-5.698	0.241	-34.453	0.705
27	Ma-8	766885	9243812	-6.965	0.247	-42.687	0.654
28	Ma-9	756664	9243013	-6.094	0.248	-36.384	0.619
Avg.				-6.60		-40.03	
Std. Dev.				0.53		3.57	
CV				-8.01		-8.93	

term, the groundwater in the deep wells has a more homogeneous source than in the springwater.

The δ^2H and $\delta^{18}O$ contents of rainwater in different locations lead to various isotopic compositions (Clark, 2015). The local meteoric line equation is a reference line used to determine the groundwater genesis and movements, as well as processes that occur in an area (Mazor, 2004). As an attempt to identify the relationship between groundwater and meteoric water in the researched

area, the results of the isotope analysis are plotted on the local meteoric water line (LMWL) with an equation of $\delta^2H = 7.8\ \delta^{18}O + 10.3$ (Wahyudin et al., 2013).

The plots of $\delta^{18}O$ and δ^2H in groundwater samples against the local meteoric water line (LMWL) can be seen in Figure 10. Groundwater samples located close to the LMWL represent modern groundwater (Li et al., 2013). The plots of groundwater samples from deep wells and
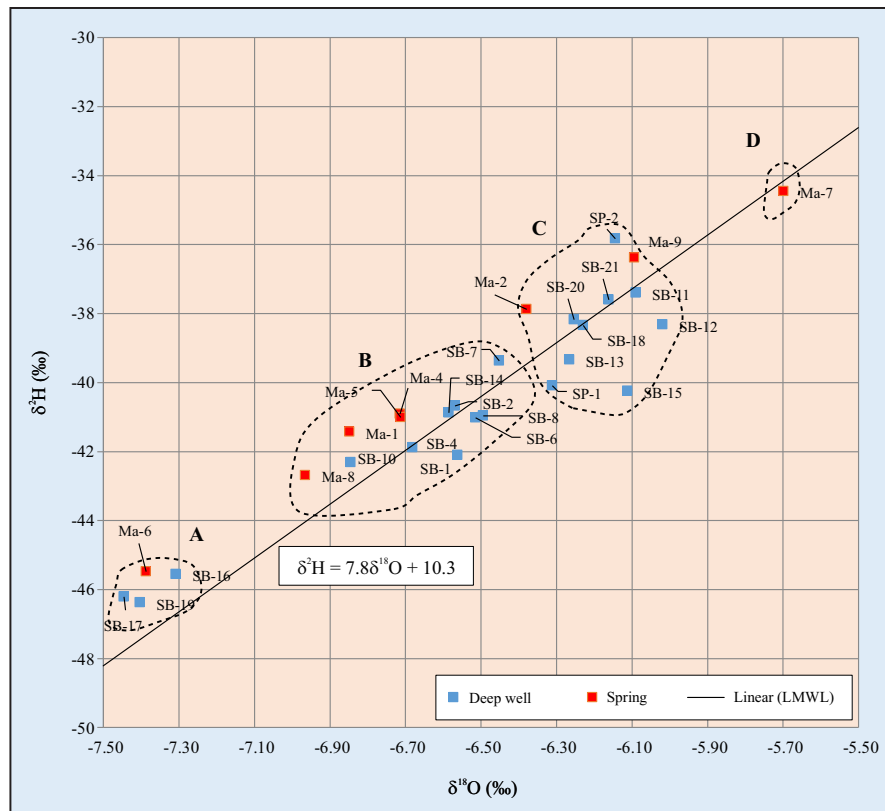
Figure 10. Plots of δ^2H *vs*. $\delta^{18}O$ values of water samples representing modern groundwater and showing four groups with similar of $\delta^{18}O$ and δ^2H values.

springs on the LMWL show four groups with similar $\delta^{18}O$ and δ^2H composition, namely water samples with light (Group A), light to moderate (Group B), moderate to heavy (Group C), and heavy composition (Group D) (Figure 10).

The groundwater samples in Group A, *i.e.* relatively light $\delta^{18}O$ and δ^2H compositions, are found in SB-16, SB-17, SB-19, and Ma-6, with ^{18}O levels varying between -7.45 and -7.31‰ and ^2H ranging from -46.38 to -45.48‰. Group B (light to moderate $\delta^{18}O$ and δ^2H compositions) is detected in SB-1, SB-2, SB-4, SB-6, SB-7, SB-8, SB-10, SB-14, Ma-1, M- 4, Ma-5, and Ma-8, with $\delta^{18}O$ contents of -6.97 to -6.45‰ and δ^2H of -42.69 to -39.38‰. Group C (moderate to heavy ^{18}O and ^2H compositions) is identified in SP-1, SP-2, SB-11, SB-12, SB-13, SB-15, SB-18, SB-20, SB-21, Ma-2, and Ma-9, with the $\delta^{18}O$ compositions ranging from -6.38 to -6.02‰ and δ^2H from -40.25 to -35.83‰. As for Group D (high $\delta^{18}O$ and δ^2H compositions), it is discovered in Ma-7, with -5.70‰ $\delta^{18}O$ and -34.45‰ δ^2H. This

groundwater sample was collected from a spring in the hill in the northwest of the studied area.

DISCUSSION

The identification of the hydrogeological system in this study is based on lithological and stratigraphic analyses and the δ^2H and $\delta^{18}O$ compositions of the groundwater samples. The stable isotope analysis reveals an irregular pattern and local groundwater recharge and discharge, which typify the complexity of the hydrogeological system. The plots of δ^2H and $\delta^{18}O$ on the LMWL are validated with geological maps, and the results illustrate the development of three hydrogeological zones of subgroundwater basins (Sub-GWB), namely Sub-GWB-A in the west, Sub-GWB-B in the middle, and Sub-GWB-C in the east. The δ^2H and $\delta^{18}O$ regression analysis of these three zones is depicted in Figure 11, while their spatial distribution is presented in Figure 12.
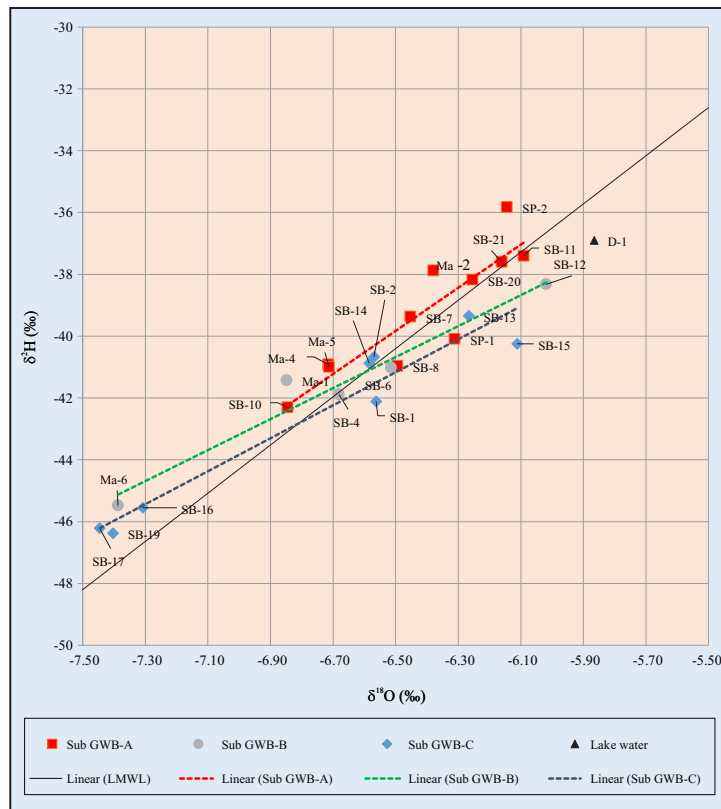
Figure 11. Linear regression analysis of the ²H and ¹⁸O showing three hydrogeological zones of subgroundwater basins in the studied area.

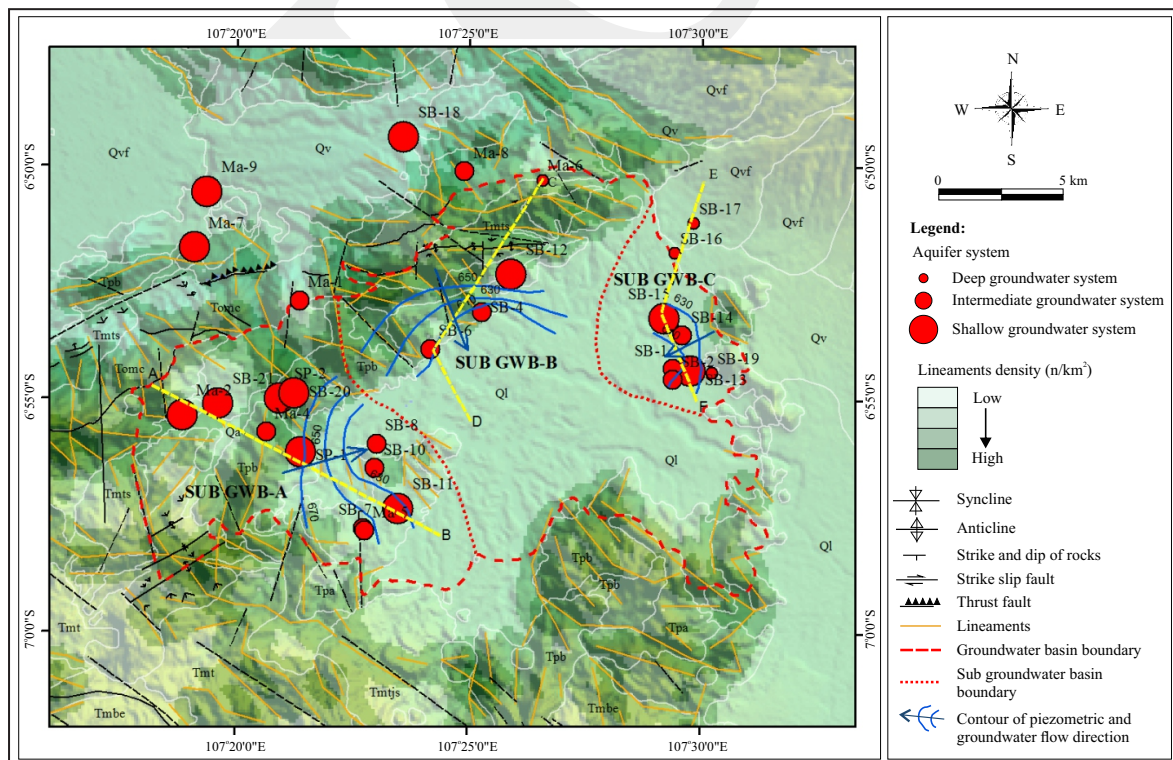Figure 12. Hydrogeological system in the studied are based on lithological and stratigraphic analyses and the δ²H and δ¹⁸O compositions of the water samples.

Subgroundwater Basin-A

The hydrogeological system in Sub-GWB-A comprises shallow and intermediate groundwater flow systems, with the groundwater flow direction relatively west-east (Figure 13). Unconfined or shallow groundwater flow systems are spread evenly both in folded sedimentary hills and undulating plain unit. These locations are the transition zone between high and low lineament densities, indicating changes in secondary porosity that eventually creates a place for groundwater accumulation. Shallow groundwater with heavy $\delta^{18}O$ and δ^2H composition, as found in MA-2, SB-20, SB-21, SP-1, SP-2, and SB-11, signifies the existence of local groundwater recharge in hills with high lineament density. The local unconfined groundwater system is connected to a geologic control, that is the northwest-southeast lineament. Its EC varies between 124 and 628 uS/cm (averagely 307 uS/cm) with Ca-HCO$_3$ (SG-1, SP-2), Ca-Na-HCO$_3$ (SG-2 and SG-3), Ca-Mg-HCO$_3$ (SP-1), Na-Ca-HCO$_3$ (SB-11), Ca-Mg-Na-HCO$_3$ (SB-20), and Ca-HCO$_3$ facies (SB-21, Ma-2). Hydrogeochemical processes like cation exchange and silicate dissolution are mostly intensive in SB-11 with an electrical conductivity of 628 uS/cm. The intermediate groundwater flow system is indicated by moderate $\delta^{18}O$ and δ^2H values, particularly in groundwater samples numbers Ma-4, Ma-5, SB-7, SB-8, and SB-10. It is located

in the northwest of the studied area, specifically at the borders between plain and hills, where the deep wells are as deep as 90 to 150 m.

The intensive interaction between groundwater and rocks is typified by EC ranging from 245 to 467 uS/cm (averagely 339 uS/cm) and Ca-HCO$_3$ (Ma-4, Ma-5), Ca-Mg-HCO$_3$ (SB-10), and Na-Ca-HCO$_3$ facies (SB-7). In SB-7, there is an enrichment of Na due to cation exchange. In addition to cation exchange, the sample also has a high rate of silicate dissolution as a sign of relatively long residence time in sandstone aquifers. Accordingly, the hydrochemical properties in both shallow and intermediate groundwater systems were shaped by the same processes, namely cation exchange and dissolution of silicate minerals, which occur most intensively in SB-11 (shallow aquifer system) and SB-7 (intermediate aquifer system).

Subgroundwater Basin-B

The hydrogeological system in Sub-GWB-B is divided into shallow and intermediate-to-deep groundwater flow systems, with the groundwater flow direction relatively northwest-southeast (Figure 14). The shallow or unconfined groundwater flow system is spread locally at the interface between folded sediment hills and undulating plain unit. Unconfined aquifer system with local groundwater recharge is found not only in shallow
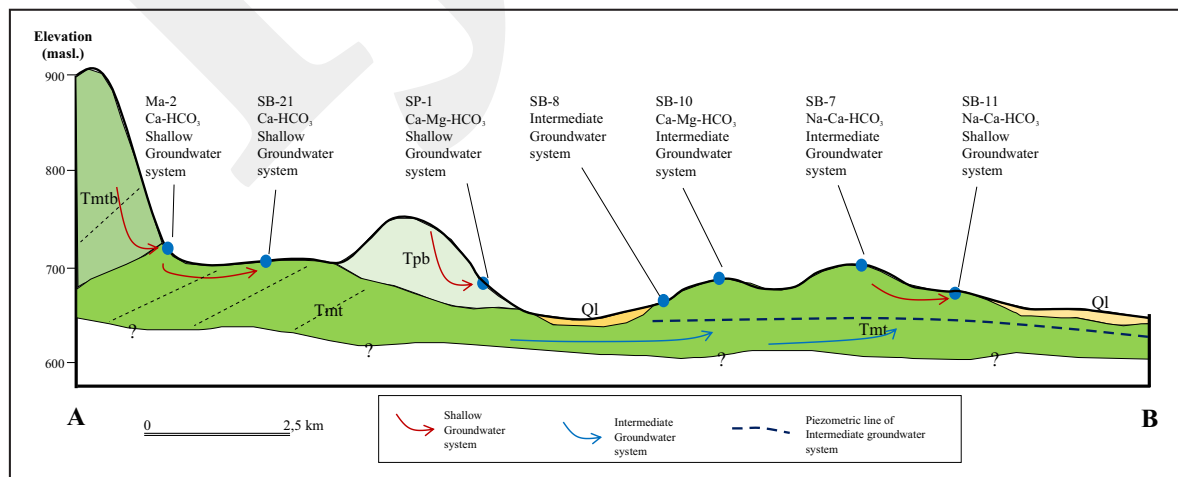

Figure 13. Cross-section of the hydrogeological system in Sub-GWB-A showing the shallow and intermediate groundwater flow systems.
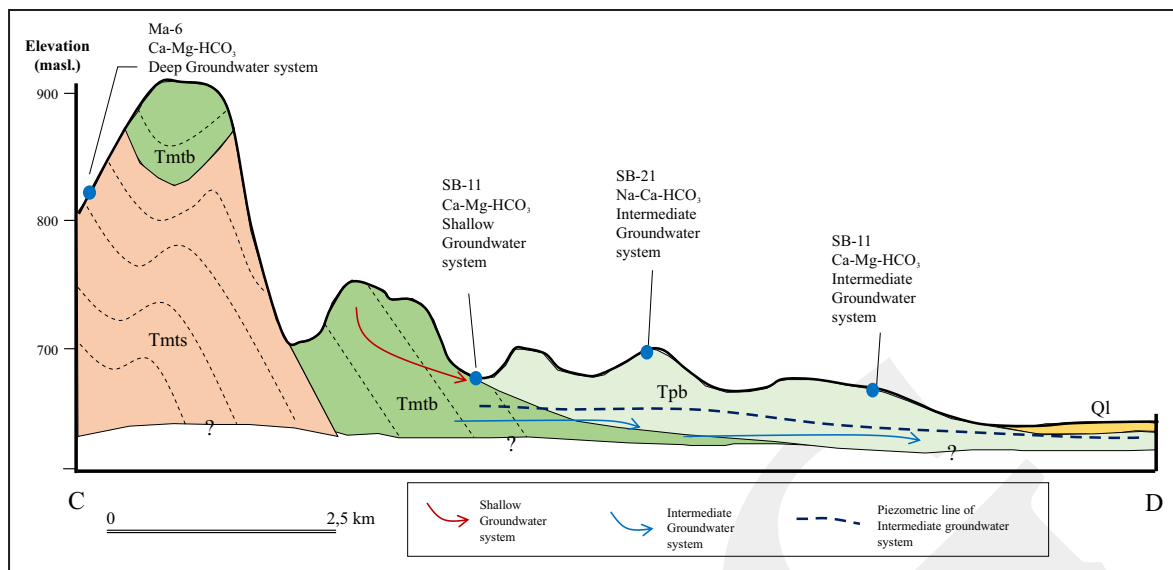
Figure 14. Cross-section of the hydrogeological system of Sub-GWB-B showing shallow and intermediate-to-deep groundwater flow systems.

wells, but also in deep wells at a depth of 55 m (*e.g.* SB-12). The recharge area of groundwater in this zone is likely the hill upstreams that have a northeast-southwest direction and high lineament density. The level of interaction between groundwater and rocks is indicated by EC of 403 uS/cm with Mg-Na-HCO$_3$ facies in SB-12 and EC of 490 uS/cm with Ca-Mg-HCO$_3$ facies in SG-4, which are the results of silicate dissolution and cation exchange. The intermediate to deep groundwater flow system is distributed in the northwest to the north of the studied area, as signified by the moderate composition of $\delta^{18}O$ and δ^2H in Ma-1, SB-4, and SB-6, and the lowest one in Ma-6. The depth of the deep wells is about 90 to 150 m, which is located in a reverse fault between tuffaceous breccia intercalated with sandstone and conglomerate (Pb) and the breccia and sandstone members of the Citarum Formation (Mtb).

The intensive interaction between groundwater and rocks is identified from relatively high electrical conductivities, which are 306 uS/cm (Ma-1), 520 uS/cm (SB-4), 472 (SB-6), and 198 (Ma-6). The hydrochemical facies also vary, including Ca-Mg-HCO$_3$ (Ma-1 and Ma-6), Na-Ca-HCO$_3$ (SB-4), and Ca-Na-Mg-HCO$_3$ (SB-6). Intensive hydrogeochemical processes like cation exchange and dissolution of silicate minerals

taking place in SB-4 and SB-6, demonstrate a relatively long residence time in the aquifer.

Subgroundwater Basin-C

There are two groundwater flow systems in Sub-GWB-C, namely shallow and intermediate-to-deep with the groundwater flow direction relatively northeast-southwest (Figure 15). Unconfined aquifer systems with shallow groundwater flow are represented by groundwater samples numbers SB-13 and SB-15 that have relatively heavy δ^2H and $\delta^{18}O$ composition, expressing the presence of local recharge system. This aquifer system has no indications of lineament control or, in other words, porous media dominantly shapes the groundwater flow. The top layer of the aquifer is composed of lake deposits, while the bottom is of tuffaceous breccia (Pb). The effects of evaporation are apparent in groundwater in SB-15, which is believed to have interacted with surface or lake water. Intensive groundwater-rock interaction is evident of the relatively high EC, namely 651 uS/cm in SB-13 and 558 uS/cm in SB-15. The Ca-Na-HCO$_3$ facies in SB-13 and Ca-Na-Mg-HCO$_3$ facies in SB-15 suggest that the dominant hydrogeochemical processes are intensive cation exchange and silicate dissolution. Groundwater samples from SB-1, SB-2, and SB-14 represent
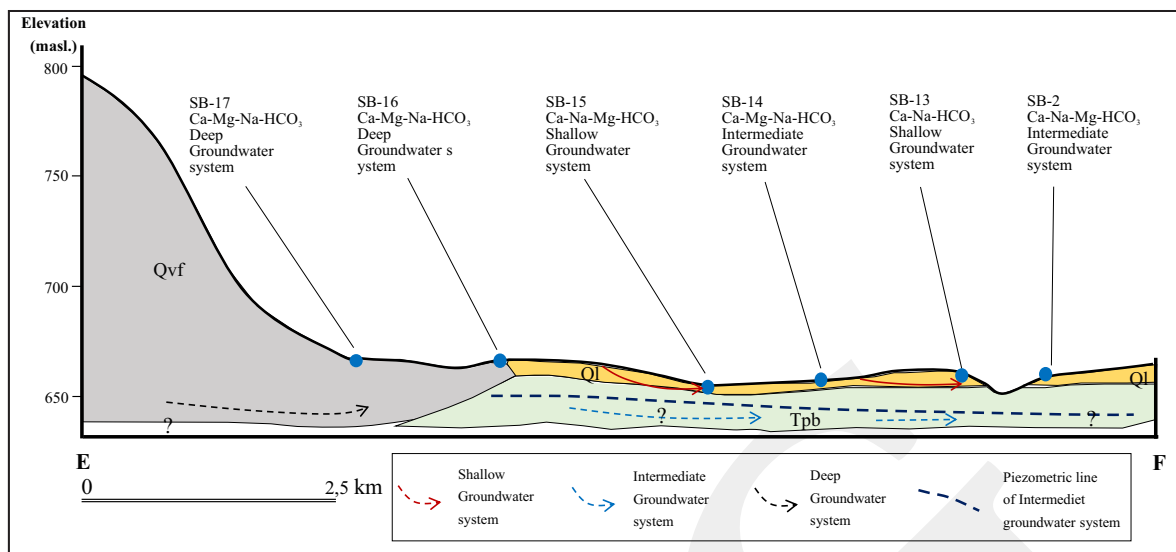
Figure 15. Cross-section of the hydrogeological system of Sub-GWB-C showing shallow and intermediate-to-deep groundwater flow systems.

groundwater flow system with medium ^{2}H and ^{18}O compositions.

The intensive groundwater-rock interaction is reflected by the relatively high electrical conductivities, namely 549 uS/cm (SB-1), 368 uS/cm (SB-2), and 541 uS/cm (SB-14) with hydrochemical facies of Ca-Mg-HCO$_3$ (SB-1), Ca-Na-Mg-HCO$_3$ (SB-2), and Ca-Mg-Na-HCO$_3$ (SB-14).The deep groundwater system can be found in SB-16, SB-17, and SB-19. These deep wells have the light δ^2H and δ^{18}O composition, which show that the groundwater is recharged from the highest elevation in the northeastern part of this area. The dominant lithology of this aquifer system is tuffaceous breccias (Pb) overlain by lake deposits (Ql) that are bordered by laharbreccias (Qyg), and SB-17 is located in these lahar breccias (Qyg). An intensive groundwater-rock interaction is also represented by electrical conductivities of 247 uS/cm (SB-16), 208 uS/cm (SB-17), and 218 uS/cm (SB-19), with hydrochemical facies of Ca-Mg-Na-HCO$_3$ (SB-16 and SB-17) and Ca-Mg-Na-HCO$_3$-Cl (SB-19). The hydrogeochemical processes taking place in this system are intensive cation exchange and silicate dissolution.

The explanation above shows that in the Sub-GWB-C, the unconfined aquifer systems have a higher electrical conductivity and more intensive cation exchange and silicate dissolution than intermediate and deep aquifer systems. These characteristics reflect a prolonged interaction between groundwater and the aquifer system underneath. Unconfined or shallow groundwater system has a lower hydraulic conductivity than intermediate-to-deep groundwater flow system; hence, prolonged residence time. Although deep aquifers have lower electrical conductivity than shallow and intermediate ones, they are subjected to more intensive cation exchange and silicate rock dissolution compared to intermediate aquifer systems. The deepest aquifer is withdrawn through deep wells with depths of 104, 150, and 120 m. For this reason, the groundwater system has a further recharge area, which possibly has the same system as the Bandung-Soreang Groundwater Basin.

Based on the hydrochemical and stable isotope analyses as described above, the groundwater of the studied area has generally shown hydrochemical evolution from Ca^{2+} to Mg^{2+} then Na$^+$ as the consequence of cation exchange and dissolution of silicate minerals. However, there have been no signs of anion evolution, meaning that HCO$_3^-$ still prevail the groundwater types in the studied area. According to Sophocleous (2004), these conditions refer to a local groundwater system. A local groundwater system has recharge areas at a

high topography, and is bordered directly by the discharge area at low terrains (Freeze and Cherry, 1979; Fetter, 1994; Toth, 2009). Although the groundwater system in the studied area is local, it has three relative systems, namely shallow, intermediate, and deep groundwater flows that are segmented in three subgroundwater basins. The results of this study also indicate that in areas composed of Tertiary sedimentary rocks that are compact and tend to be impermeable, it can still function as a groundwater recharge area. The morphological lineaments, hydrochemical, and stable isotope analyses show that the fracture system plays an important role as a connector between the recharge system in hilly areas and the discharge system in plain areas.

Conclusions

The groundwater flow pattern in the studied area is controlled by the northwest-southeast morphological lineament, which is represented by the emergence of springs at the borders between the high-and low-density zones. In order of dominance, the groundwater facies is as follows: $Ca-Mg-HCO_3>Ca-HCO_3>Ca-Na-Mg-HCO_3>Na-Ca-HCO_3$. As evident from the bivariate analysis, the dominant hydrogeochemical processes are the dissolution of silicate minerals and cation exchange. The most intensive processes have been identified in water samples numbers SB-7, SB-11, SB-3, SB-6, and SG-4, meaning that the groundwater has prolonged residence time in the aquifer. Hydrochemical evolutions are apparent from Ca^{2+} to Mg^{2+} then Na^+, which are caused by cation exchange and dissolution of silicate minerals. Since there is no indication of anion changes, HCO_3^- still dominates the groundwater facies, and it also represents a local groundwater flow system. Based on the geological and hydrogeochemical analyses, as well as stable isotope composition, the studied area is broadly divided into three subgroundwater basins (Sub-GWB), namely Sub-GWB-A in the west, Sub-GWB-B in the middle, and Sub-GWB-C in the east. Aquifer

systems with shallow to intermediate groundwater flow exist in all subgroundwater basins, while deep groundwater flow systems can be found in Sub-GWB-B and Sub-GWB-C. Fracture system has an important role as a connector between the recharge system in hilly areas and discharge system in plain areas.

References

Anonymous, 2017. *Peraturan Menteri ESDM No. 2 Tahun 2017 Tentang Cekungan Air Tanah di Indonesia.* Kementerian Energi dan Sumber Daya Mineral.

Al Charideh, A., 2011. Geochemical and isotopic characterization of groundwater from shallow and deep limestone aquifers system of Aleppo Basin (northern Syria). *Environmental Earth Sciences*, 65, p.1157-1168. DOI: 10.1007/s12665-011-1364-6

van Bemmelen, R.W., 1949. *The Geology of Indonesia, Part I General Geology*. The Hague, Netherland.

Clark, I., 2015. *Groundwater geochemistry and isotopes*.CRC Press.

Dam, M.A.C. and Suparan, P.,1992. *Geology of the Bandung Basin*. Report with the 1:50.000 Quaternary Geological Map of the Bandung Basin, Geological Research and Development Centre, Bandung.

Dam, M.A.C.,1994. *The Late Quaternary Evolution of The Bandung Basin, West Java, Indonesia*. Department or Quaternary Geology,

Faculty of Earth Sciences,Vrije Universiteit, De Boele Laan 1085, Amsterdam.

Delinom, R.M., 2009. Structural Geology Controls on Groundwater Flow: Lembang Fault Case Study, West Java, Indonesia. *Hydrological Journal,* 17 (4), p.1011-1023, Springer Verlag, 2009, Germany. DOI: 10.1007/s10040-009-0453-z

Eriksson, E., 1983. Stable Isotopes and Tritium in Precipitation, Guide Book on Nuclear Techniques in Hydrology. *Technical Report Series No. 91*, IAEA, Vienna.

Gaillardet, J., Dupre, B., Louvat, P., and Allegre, C.J., 1999. Global silicate weathering and CO_2 consumption rates deduced from the chemistry of large rivers. *Chemical Geology*, 159, p.3-30. DOI: 10.1016/S0009-2541(99)00031-5

Geyh, M.A., 1991. Isotopic Hydrological Study in the Bandung Basin Indonesia. Laporan-Penelitian.

Gibbs, R.J., 1970. Mechanisms controlling world water chemistry. *Science*, 170 (3962), p.1088-1090. DOI: 10.1126/science.170.3962.1088

Fetter, C.W., 1994. *Applied Hydrogeology*. Prentice-Hall, Inc., New Jersey, 598pp.

Fetter, C.W., 2001. *Applied Hydrogeology. 4th Edition*, Prentice-Hall, New Jersey.

Freeze, R.A. and Cherry, J.A., 1979. *Groundwater*. Prentice-Hall, New Jersey, 604pp.

Hem, J.D., 1992.Study and interpretation of the chemical characteristics of natural waters. US Geological Survey, *Water-Supply Paper 2254*.

IWACO and Waseco,1991. *Studi Hidrologi Bandung*, Laporan Utama Tambahan 2. Sumberdaya Airtanah,West Java Provincial Water Sources Master Plan or Water Supply.

Kehew, A.E., 2001. *Applied Chemical Hydrology*, Prentice-Hall, New Jersey.

Kim, G.B., 2003. *Construction of a Lineament Density Map with Arc View and Avenue*. Korea Water Resource Corporation, South Korea.

Koesoemadinata, R.P. and Hartono, D., 1981. Stratigrafi dan Sedimentasi Daerah Bandung.

Proceedings of Indonesian Association of Geologist Annual Conference, X, Bandung, p.318-336.

Koesmono, 1976. *Peta Geologi Lembar Sindangbarang*, *Jawa*. Direktorat Geologi, Departemen Pertambangan. R. I. Bandung.

Koesmono, Kusnama, and Suwarna, N., 1996. *Peta Geologi Lembar Sindangbarang, Jawa, Skala 1:100.000,* 2nd Edition. Pusat Penelitian dan Pengembangan Geologi, Bandung.

Li, J., Liu, J., Pang, Z., and Wang, X., 2013. Characteristics of Chemistry and Stable Isotopes in Groundwater of the Chaobai River Catchment, Beijing. *Procedia Earth Planetary Science,* 7, p.487-490. DOI: 10.1016/j.proeps.2013.03.092.

Mandel, S. and Shiftan, Z., 1981. *Groundwater Resources. Investigation and Development*, Academic Press, New York.

Matahelumual, B.C. and Wahyudin, 2010. *Penelitian Hidrogeologi Daerah Imbuhan Air Tanah Dengan Metode Isotop dan Hidrokimia di Cekungan Air Tanah Bandung-Soreang, Provinsi Jawa Barat (Tahap III)*. Pusat Lingkungan Geologi, Badan Geologi, Bandung.

Mazor, E. 2003. Chemical and Isotopic Groundwater Hydrology, 3rd Edition. Boca Raton: CRC Press, 352pp. DOI: 10.1201/9780203912959

Schoeller, H.,1977. Geochemistry of groundwaters. *In*: *Groundwater studies-an international guide for research and practice*. UNESCO, Paris, p.1-18.

Schwartz, F.W. and Zhang, H., 2003. *Fundamentals of Groundwater*, John Wiley & Sons, New York.

Silitonga, P.H., 1973. *Peta Geologi Lembar Bandung, Jawa, Skala 1:100.000*. Pusat Penelitian dan Pengembangan Geologi.

Singhal, B.B.S. and Gupta, R.P., 1999. *Applied Hydrogeology of Fractured Rocks*. Kluwer Academic Publisher, Netherlands, 415pp.

Sophocleous, M.A., 2004. Groundwater recharge and water budgets of the Kansas High Plains and related aquifers. *Kansas Geological Survey Bulletin,* 249, p.1-102.

Sudjatmiko, 1972. *Peta Geologi Lembar Cianjur-9/XIII-E, Jawa Barat.* Pusat Penelitian dan Pengembangan Geologi, Bandung.

Sudjatmiko, 2003. *Peta Geologi Lembar Cianjur, Jawa, Skala 1:100.000.* Pusat Penelitian dan Pengembangan Geologi, Bandung.

Sunarwan, B., 1997. *Penerapan Metode Hidrokimia-Isotop Oksigen (^{18}O), Deuterium (^{2}H) dan Tritium (^{3}H), dalam Karakterisasi Akuifer Air Tanah pada Sistem Akuifer Bahan Vulkanik. Studi Kasus: Kawasan Padalarang-Cimahi, Bandung.* Tesis Magister Program Studi Teknik Geologi ITB.

Sutrisno, S., 1983. *Peta Hidrogeologi skala 1:250.000, Lembar Bandung.* Direktorat Geologi Tata Lingkungan, Bandung.

Todd, D.K., 1984. *Groundwater Hydrology*, John Wiley & Sons, 552pp.

Toth, J., 2009. *Gravitational systems of groundwater flow: theory, evaluation, utilization.* Cambridge University Press. DOI: 10.1017/CBO978051157654.

Wahyudin, Mattahelumual, B.C., Dijono, and Satriyo, 2013. Karakteristik Isotop dan Hidrokimia Pada Sistem Aliran Air Tanah Daerah Bandung dan Sekitarnya. *Majalah Geologi Indonesia*, 24 (2), p.117-128.

Wang, H., Jiang, X.W., Wan, L., Han, G., and Guo, H., 2015. Hydrogeochemical characterization of groundwater flow systems in the discharge area of a river basin. *Journal of Hydrology,* 527, p.433-441. DOI: 10.1016/j.jhydrol.2015.04.063

Wu, J., Li, P., Qian, H., Duan, Z., and Zhang, X., 2013. Using correlation and multivariate statistical analysis to identify hydrogeochemical processes affecting the major ion chemistry of waters: a case study in Laohebaphosphorite mine in Sichuan, China. *Arabian Journal Geosciences*. DOI: 10.1007/s12517-013-1057-4.

Yuan, J., Xu, F., Deng, G., Tang, Y., and Li, P., 2017. Hydrogeochemistry of Shallow Groundwater in a Karst Aquifer System of Bijie City, Guizhou Province. *Water,* 9 (8), 16pp. DOI: 10.3390/w9080625